Supplementary Information (SI)

Papain functionalized Prussian blue nanozyme colloids of triple enzymatic function

*Attila Voros, Tibor G. Halmagyi, Szilard Saringer, Viktoria Hornok, Istvan Szilagyi**

MTA-SZTE Momentum Biocolloids Research Group, Department of Physical Chemistry and Materials Science, Interdisciplinary Centre of Excellence, University of Szeged, 1 Rerrich Béla tér, 6720 Szeged, Hungary

*Corresponding author. Email: szistvan@chem.u-szeged.hu

Experimental Section

Materials. Folin-Ciocalteu reagent (2 N solution), hydrogen peroxide (approx. 31 wt %), and papain (PPN, extracted from *Carica Papaya*, ≥ 3 U/mg) were purchased from Sigma-Aldrich. Calcium chloride (reagent grade), casein, guaiacol (99 %), hydrogen chloride (37 wt %), L(-)-tyrosine (99 %), magnesium chloride hexahydrate (99 %), nitro blue tetrazolium chloride monohydrate (NBT, ≥ 98 %), polyvinylpyrrolidone (PVP, M_w approx. 50 g/mol), potassium chloride (99.5 %), potassium hexacyanoferrate(III) (99 %), sodium chloride (99.8 %), sodium hydroxide (98.5 %), monobasic sodium phosphate (reagent grade), dibasic sodium phosphate (reagent grade) and trichloroacetic acid (TCA, 99.5 %) were procured from VWR. An Adrona water purification system was used for producing ultrapure water, which was filtered prior sample preparation for light scattering measurements with a 100 nm pore size Millex syringe filter.

Synthesis of PB Nanocubes. PB nanocubes were synthesized via a polymer-templating method adapted from literature.[1, 2] In brief, solutions of PVP and potassium hexacyanoferrate(III) were mixed together and sirred at 80 °C for at least 20 hours. The resulting blue dispersion was then washed several times with pH 4 HCl solution and ethanol followed by centrifugation. The nanoparticles were re-suspended in filtered ultrapure water and the pH was adjusted to 4 by addition of HCl solution.

PPN Enzyme Immobilization. A mixture of 400 ppm PB and 100 ppm PPN was prepared, and left to equilibrate over 30 minutes. The resulting PB-PPN stock dispersions were used directly in subsequent experiments. Throughout the text, PB-PPN concentration values denote the concentration of PB in the mixture. For the dosing experiments, varying concentrations of PPN were added to the 400 ppm PB dispersion but the method otherwise remained identical to the one described above.

Bradford Test on PB-PPN. The amount of free PPN in the PB-PPN mixture was determined with the Bradford protein assay.[3, 4] Coomassie Brilliant Blue (CBB) stock solution was prepared by dissolving 10 mg CBB in a mixture of 5 mL ethanol and 10 mL 85 % phosphoric acid. The solution was then diluted to 100 mL with ultrapure water. The test itself was performed by first preparing 0-8 ppm PPN calibration solutions, 0.4 mL of which were then mixed with 1.6 mL CBB solution. After 5 min of equilibration time, UV-visible spectra were recorded between 400-800 nm. An assay of 40 ppm PB-PPN concentration was also performed in the same way. By measuring absorbance values of the calibration series as well as of the PB-PPN assay at 595 nm, the free PPN concentration in PB-PPN could be determined.

Dynamic Light Scattering (DLS). 3D modulated cross-correlation DLS measurements were performed on a 3D LS Spectrometer (LS Instruments, Switzerland) equipped with a 633 nm He-Ne laser of 120 mW maximum power. Measurements were performed at a 150° scattering angle (θ). Cumulant fits of the intensity autocorrelation curves yielded the diffusion constant (D) of the particles, from which the hydrodynamic radii (R_h) of the particles were calculated using the Stokes-Einstein equation as[5]

$$R_h = \frac{k_B T}{6\pi\eta D} \tag{S1}$$

where k_B is Boltzmann's constant, T is the absolute temperature, and η is the dynamic viscosity. It needs to be noted that hydrodynamic radius values are often larger than the radius of the solid particle, as R_h represents the radius of a sphere that diffuses at the same rate as the particle in dispersions.[6] Size distributions were evaluated with the LS Instruments proprietary CORENN sizing algorithm.

Electrophoretic Light Scattering (ELS). ELS experiments were performed on an Anton Paar Litesizer 500 light scattering instrument equippped with a 40 mW laser of 685 nm, at 15° scattering angle. Anton Paar Omega cuvettes with gold-coated electrodes were used in all experiments.

SOD Assay. Superoxide dismutase activity of the nanozymes was characterized with a modified version of the Fridovich assay.[7] In this assay, the superoxide is produced via the oxidation of xanthine with the xanthine oxidase enzyme. In the absence of a SOD-like catalyst, this superoxide then oxidizes a tetrazole dye (NBT) to blue-colored formazan. If a SOD-like nanozyme is present, the superoxide is scavenged before oxidizing the NBT thus the color change is suppressed. In a typical assay, a mixture of 200 µM xanthine, 100 µM NBT and 0 - 100 ppm nanozyme was prepared in 10 mM phosphate buffer (pH 6.9). 300 ppm xanthine oxidase was added to initiate the oxidation of xanthine to uric acid, producing superoxide. The subsequent oxidation of NBT was monitored with UV-visible spectrophotometry at 565 nm for 6 minutes. The activity of the nanozyme was defined as its ability to inhibit the increase of solution absorbance from formazan formation as

$$I = \frac{\Delta A_0 - \Delta A_s}{\Delta A_0} \cdot 100\% \qquad \text{(S2)}$$

where ΔA_0 is the change in absorbance over 6 minutes in the „control" solution with 0 ppm nanozyme, and ΔA_S is the absorbance change of a sample with a given nanozyme concentration. Inhibition (I) versus time curves were then constructed and the 50 % inhibition concentration (IC_{50}) was calculated from a multi-parametric nonlinear fit. The error of this assay is 10 %.

POD Assay. A method utilizing the guaiacol substrate was adapted from literature for the determination of the POD-like activity of the nanozymes.[8] In a typical measurement, 40 ppm nanozyme was added to a solution containing 0-40 mM guaiacol and 50 mM phosphate buffer (pH 6.9). The reaction was initiated by the addition of 2.7 mM H_2O_2 and the change in absorbance at

470 nm was monitored. The reaction rate (v) was determined from the absorbance versus time plots and plotted against the guaiacol concentration and fitted with the Michaelis-Menten model as

$$v = \frac{v_{max} \cdot [S]}{K_M + [S]} \quad \text{(S3)}$$

where v_{max} is the maximum initial reaction rate, $[S]$ is the substrate concentration, and K_M is the Michaelis constant indicating the affinity of the substrate to the nanozyme. A 10 % experimental error is included in this assay.

PRT Assay. The Lowry assay was adapted from literature to determine the protease activity of PB-PPN and free PPN.[9] In the Lowry assay, a cuprous complex is formed with the peptide bonds of amino acid residues. The sensitivity of this reaction is increased by the addition of the Folin-Ciocalteu reagent which interacts with the Cu^+ ions and tyrosine producing a blue-green colored complex. In a typical assay, 100 µL enzyme stock solution (100 ppm PPN or 400 ppm PB-PPN in 2 mM sodium/calcium acetate (Na:Ca was 2:1) and 4 mM potassium phosphate, pH 7.5) was added to 500 µL of casein stock solution (containing 6.5 g/L casein in 50 mM potassium phosphate buffer, pH 7.5). A blank was also prepared from 100 µL enzyme stock and 500 µL ultrapure water. After 20 minutes, 0.5 mL 110 mM trichloroacetic acid was added to each vial and the mixtures were incubated at 37 °C for 30 minutes. The samples were then centrifuged at 10000 rpm for 10 minutes to remove the dispersed nanoparticles. The supernatant was removed and a new mixture was prepared from 1 mL supernatant and 0.75 mL 0.5 M sodium carbonate. After addition of the sodium carbonate, the solutions were centrifuged again to remove the formed cloudy precipitate. 0.1 mL 0.5 M Folin-Ciocalteu reagent was added, then the samples were mixed thoroughly and left to equilibrate at 37 °C for 30 minutes. The color change upon completion of the reaction was measured with UV-visible spectrophotometry. Absorbance spectra were taken between 400-800

nm and absorbance values at 660 nm were compared to those of a tyrosine calibration series prepared similarly to the samples described above.[10]

UV-Visible Spectrophotometry. All UV-visible spectrophotometry measurements were performed in absorbance mode on a GENESYS 10S spectrophotometer procured from Thermo Scientific. Measurements were performed in disposable PMMA or PS cuvettes. All sample spectra were compared to their corresponding blanks.

Transmission Electron Microscopy (TEM). TEM images of both PB and PB-PPN nanoparticles were recorded by a Jeol JEM-1400Plus instrument (Japan) at 120 keV accelerating voltage. Before each measurement, 10 μL sample aliquots were deposited onto carbon-coated Formvar foil 200 mesh copper grids and dried. For size distribution evaluation, at least 150 particles were measured for each sample with the ImageJ program.

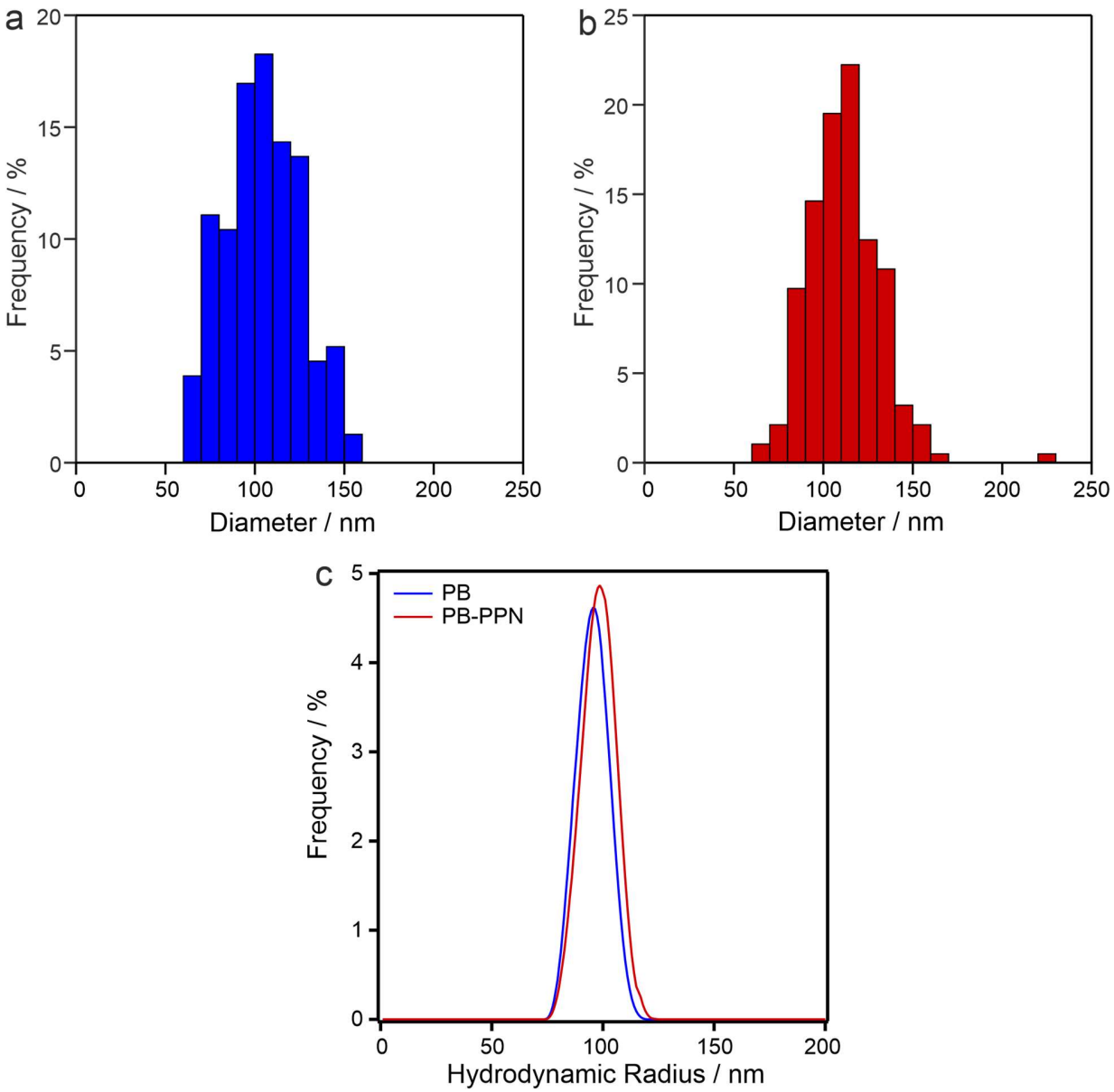

Figure S1. Size distribution of PB (a) and PB-PPN (b) obtained from TEM images. Hydrodynamic radius distribution of PB and PB-PPN determined in DLS measurements at 40 ppm particle concentration and pH 4 (c).

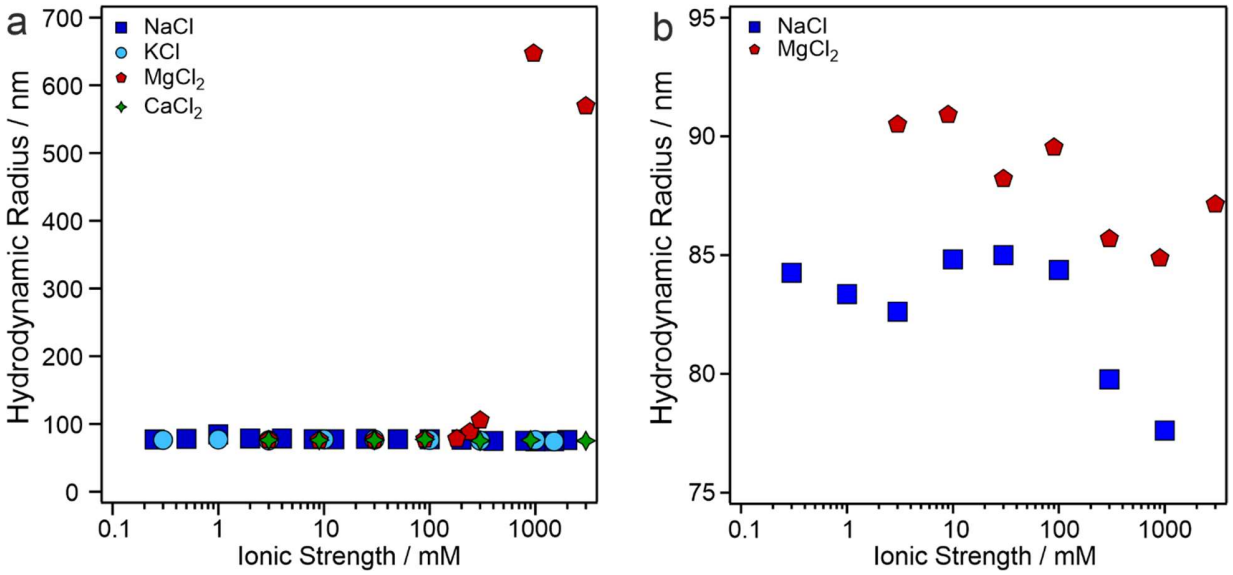

Figure S2. DLS hydrodynamic radius values of PB in various electrolytes as a function of the ionic strength (a). Hydrodynamic radius data of PB-PPN in NaCl and $MgCl_2$ versus the ionic strength (b). Data shown are average values of 10 measurements performed at 40 ppm particle concentration and pH 4.

REFERENCES

1. S. L. Wang, H. Yan, Y. L. Wang, N. Wang, Y. L. Lin and M. Li, *Microchim. Acta*, 2019, **186**, 738.
2. M. Hu, S. Furukawa, R. Ohtani, H. Sukegawa, Y. Nemoto, J. Reboul, S. Kitagawa and Y. Yamauchi, *Angew. Chem.-Int. Edit.*, 2012, **51**, 984-988.
3. M. M. Bradford, *Anal. Biochem.*, 1976, **72**, 248-254.
4. T. Zor and Z. Seliger, *Anal. Biochem.*, 1996, **236**, 302-308.
5. P. A. Hassan, S. Rana and G. Verma, *Langmuir*, 2015, **31**, 3-12.
6. J. Stetefeld, S. A. McKenna and T. R. Patel, *Biophys. Rev.*, 2016, **8**, 409-427.
7. C. Beaucham and I. Fridovich, *Anal. Biochem.*, 1971, **44**, 276-287.
8. N. B. Alsharif, G. F. Samu, S. Sáringer, S. Muráth and I. Szilagyi, *J. Mol. Liq.*, 2020, **309**, 113066.
9. S. Sáringer, T. Valtner, Á. Varga, J. Maléth and I. Szilagyi, *J. Mat. Chem. B*, 2022, **10**, 2523-2533.
10. C. Cupp-Enyard, *J. Vis. Exp.*, 2008, **19**, e899.